ESR Study on Segmental Motion of Polyethylene in Amorphous Region, Dependent on Crystallinity, Molecular Weight, and Labeled Site

Katsuhiro Yamamoto,*,† Kazumichi Kato, Yusuke Sugino,† Shigeo Hara,† Yohei Miwa,† Masato Sakaguchi,‡ and Shigetaka Shimada†

Graduate School of Engineering, Department of Materials Science & Engineering, Nagoya Institute of Technology, Gokiso-cho, Showa-ku, Nagoya 466-8555, Japan, and Nagoya Keizai University, 61 Uchikubo, Inuyama 484-8503, Japan

Received January 11, 2005; Revised Manuscript Received April 7, 2005

ABSTRACT: The transition temperature of high-density polyethylene (PE), low-density PE, and hydrogenated poly(butadiene), which was detected by the spin-labeled ESR method, was evaluated. The detected transition corresponded to the β transition of semicrystalline polymer PE. The transition temperature was found to depend on the crystallinity, the molecular weight of the sample, and labeled site. The β relaxation around chain-end segments was observed by the selective spin-labeling method. The mobility of the end segment as well as the inner segments was revealed to depend on the molecular weight (M_n) of the sample. The motional length scale (cooperative segment length) ξ of amorphous PE at T_g was estimated to be around 2 nm, which was the same order as the reported ξ for various polymers and the Kuhn length of PE.

Introduction

The relaxations of polyethylene including the linear and branched one have been extensively investigated by many researchers, and the experimental results have been reviewed.[1−5] The glass transition temperature T_g of PE was studied by X-ray diffraction,[6] Raman spectroscopy,[7] DSC using long alkyl chain as a model of PE,[7] dynamic mechanical measurement, ESR,[8] positron annihilation measurement,[9] and dielectric[10,11] and fluorescent probe measurements.[11] In other ways, the extrapolation of T_g data of a series of polyether was regarded to be the T_g of fully amorphous PE. The glass transition temperature of PE is dependent on the measurements, and as for β and γ transitions, they have been a controversial issue. In the present paper, we do not take notice of which transitions are true glass transition but take into consideration the existence of a crystalline in a sample. There are many reports considering the effect of a crystalline on glass transition and chain mobility. Boyer investigated an apparent double glass transition in various semicrystalline polymers.[12] Kanaya revealed the different non-Gaussian behavior of mean displacement of segment in PE amorphous and crystalline phase by means of the incoherent elastic neutron scattering.[13] The high-pressure effect on the CH_2 reorientation in PE was investigated by NMR, which revealed that high pressure resulted in a considerable reduction of the motion that related to the increase in crystallinity.[14] The glass transition was related to segmental mobility of amorphous region that was affected by a solid phase such as a silica surface[15−17] and a hard segment in block copolymer.[18−20] A similar situation can be imagined easily in a semicrystalline polymer. Solid-state nuclear magnetic resonance (NMR) spectroscopy revealed that semicrystalline polymer, polyethylene, is composed of crystalline, amorphous, and intermediate regions.[21] It is expected that the molecular mobility in amorphous and intermediate regions attached to the crystalline be reduced by the immobile crystalline. Boyer reviewed that the glass transition temperature (T_g) of polyethylene as a function of crystallinity (X_c) by measuring the specific volume change.[5] They reported that the β-relaxation is related to the T_g and the T_g increases linearly with the X_c. (Note that α-relaxation means a crystalline relaxation in a semicrystalline polymer.)

A semicrystalline polymer has structural heterogeneity such as molecular weight, branches, crystalline, crystalline structure, crystallinity, and amorphous (loop, tie, tail, etc.). The structural heterogeneity affects the mobility in the amorphous region of the polymer, and the heterogeneity seems to make it complicated to understand the mobility. It is of importance to survey the effect of the heterogeneity on the mobility of polymer. Recently, we investigated that the chain end effect on the glass transition of PS[22] and PMMA[23] related to the segmental cooperative motion. The molecular weight dependence of the glass transition for the end chain segments was revealed, and the scale of the cooperative volume relevant to the segmental motion of PS and PMMA corresponded well to the order of Kuhn length. In addition, a site-specific spin-labeling study in a block copolymer was reported.[18] These studies evidenced the existence of the heterogeneity in the amorphous polymer and meant that ESR spin-label technique was useful and effective for this kind of study. In this paper, we address the effect of the crystallinity, molecular weight, and chain end on the segmental motion (β transition) of polyethylene in the amorphous region as studied by the ESR spin-labeling method. The transition behavior can be regarded as the β transition of fully amorphous PE. The high- and low-density polyethylene and hydrogenated 1,4-polybutadiene were used to study the crystallinity effect on the motional transition. Molecular weight dependence of the molecular motion and site-specific study on the mobility were investigated using the hydrogenated 1,4-polybutadiene.

† Nagoya Institute of Technology.
‡ Nagoya Keizai University.

10.1021/ma050062f CCC: $30.25
Published on Web 05/05/2005

Experimental Section

Materials. Polyethylene (PE high-density PE (HDPE) Sholex 6050 and low-density PE (LDPE)) was dissolved in boiling toluene, cooled to room temperature, filtered, and dried at room temperature for more than a week. 1,3-Butadiene (BD) monomer was purchased from Tokyo Chemical. BD monomer was dehydrated under reduced pressure through a molecular sieves column, purified by addition of small amount of *n*-butyllithium, and distilled into reaction vessel before use. The spin-label reagent, 4-amino-2,2,6,6-tetramethylpiperidine-1-oxyl (4-amino-TEMPO), was purchased from Aldrich and used without further purification. Maleic anhydride (MAN) (Nacali Tesque, Co., Inc.) was dissolved into benzene and recrystallized. Benzoyl peroxide (BPO) (Nacali) was purified by precipitation from chloroform solution into methanol. *p*-Toluenesulfonyl hydrizide (TSH) as a hydrogenation reagent was purified by recrystallization from a saturated methanol solution. *N*,*N*-Dicyclohexylcarbodiimide (DCC, Nacalai) as a condensation reagent was used without further purification. All solvents (toluene, methanol, chloroform, and benzene, Extra Pure Regent, Nacalai) were distilled under reduced pressure.

Sample Preparation. Poly(1,4-butadiene) (PBD) was synthesized by anionic polymerization. Toluene (1000 mL) (or hexane) dehydrated with sodium was distilled into reaction flask which was connected to a vacuum line. BD monomer (25 g) was added into the reaction flask. The polymerization was initiated by addition of *n*-butyllithium. An addition of methanol/acetic acid terminated the polymerization. To spin-label at the chain end, PBD end must be carboxylated. An addition of carbon dioxide at the end of the polymerization of BD produced the end group, −COOLi, followed by addition of acetic acid/methanol to form a carboxylic acid group. The number-averaged molecular weight (M_n) and its distribution index (M_w/M_n) were determined by SEC with standard PBD. The microstructure was analyzed by NMR in deuterated chloroform at 298 K. The M_w/M_n of all PBD was smaller than 1.10. The microstructure of PBD synthesized in toluene and hexane was the 1,2-vinyl unit of ca. 8−10% relative to the 1,4-unit. The PBD was hydrogenated with TSH as follows: The PBD (1 g) was dissolved into toluene (100 mL) with TSH (3 mol equiv to double bond in PBD). The solution was refluxed for 24 h. The hydrogenation was completed more than 99%, which was confirmed by FT-IR measurement.

Spin-Labeling. HDPE, LDPE, and hydrogenated PBD (HPB) (except for end carboxylated PBD) have no functional group to be spin-labeled with 4-amino-TEMPO. These polymers was added into benzene solution, including BPO and maleic anhydride, degassed, sealed, and heated at 333 K. These polymers were attached with succinic anhydride group. The succinic anhydride group is easily reacted with 4-amino-TEMPO in chloroform, generating an amide bond. End carboxylated PBD (E-HPB) was spin-labeled with 4-amino-TEMPO using DCC in toluene at 273 K for 48 h. After labeling, the sample were washed with acetone by Soxhlet extraction for 24 h and dried in a vacuum desiccator.

Measurement. NMR was performed on a Bruker AVANCE 200 spectrometer using deuterated chloroform at 298 K with tetramethylsilane as an internal reference.

The M_n and M_w/M_n of the PBD were determined by GPC in THF (1 mL/min) at 313 K on four polystyrene gel columns (Tosoh TSK gel GMH (beads size is 7 μm), G4000H, G2000H, and G1000H (5 μm)) that were connected to a Tosoh CCPE (Tosoh) pump and an ERC-7522 RI refractive index detector (ERMA Inc.). The columns were calibrated against standard polybutadiene samples.

Each sample was contained in a quartz tube, and the tube was depressurized to a pressure of 10^{-4} Torr and sealed before ESR measurement. ESR spectra at 77 K and higher temperatures were observed at low microwave power level to avoid power saturation and with 100 kHz fielded modulation using JEOL JES-FE3XG and JES-RE1XG spectrometers (X band) coupled to microcomputers (NEC PC-9801). The signal of 1,1-diphenyl-2-picrylhydrazyl (DPPH) was used as a *g* tensor standard. The magnetic field was calibrated with the well-known splitting constants of Mn^{2+}.

A modulated temperature differential scanning calorimeter (MDSC, TA 5000) manufactured by TA Instruments was used. Modulation amplitude of 1.5 K and a period of 60 s were used at a heating rate of 2 K/min. The calorimeter was calibrated with an indium standard.

Each sample were basically annealed above melting temperature of PE unit for an hour and cooled to room temperature. As for HDPE and LDPE samples, to make its crystallinity decreased, the annealed HDPE and LDPE were quenched into ice water. The characteristics of all samples are listed in Table 1.

Table 1. Characteristics of Polyethylene

sample	$M_n \times 10^{-3}$ (M_w/M_n)	X_c (%)	T_{5mT} (ESR)	X_c (%)[a] for DSC	T_g (DSC)
LDPE[b]		34.6	310		
LDPE		49.9	313		
HDPE[b]		58.2	331		
HDPE		79.0	358		
HPB1.2	1.2 (1.09)	63.1	340	52.5	253
HPB4.7	4.7 (1.02)	50.3	347	41.3	256
HPB10	10.0 (1.03)	43.0	349	33.0	256
HPB20	20.0 (1.10)	40.3	347	40.2	262
HPB29.3	29.3 (1.02)	47.6	355	46.0	270
HPB30	30.0 (1.01)	40.0	347	37.2	260
HPB40	40.0 (1.01)	41.0	348	38.7	262
E-HPB2	2.0 (1.06)	43.0	304		
E-HPB4.2	4.2 (1.20)	48.0	322		
E-HPB5.8	5.8 (1.18)	34.0	322		
E-HPB12.6	12.6 (1.24)	40.9	322		
E-HPB23	23.0 (1.09)	33.6	323		
E-HPB23	23.0 (1.09)	30.6	321		
E-HPB29.3	29.3 (1.24)	39.7	327		

[a] Prepared independently in order to determine the T_g from DSC measurement. [b] Prepared by rapid quenching into ice water from melt sample.

The crystallinity of polyethylene X_c was determined by wide-angle X-ray diffraction that was performed at beamline BL-9C and BL-15A in Photon Factory of the High Energy Accelerator Research Organization (KEK) in Tsukuba, Japan. White radiation from the source was monochromized using a double monochromator of Si(111) crystal to give an intense beam of $\lambda = 0.1499$ nm X-rays. The detector is one-dimensional position-sensitive proportional counter (PSPC) located at a distance of 30 cm from the sample position. The polyethylene, tripalmitin, and lead stearate were used as standards to calibrate the detector. The experimental data were correlated for the background scattering and sample adsorption.

Result and Discussion

Crystallinity Dependence of Transition Temperature from ESR. Temperature-dependent ESR spectra of the HDPE and LDPE labeled at the inside segments of the chain with different crystallinity (X_c) are shown in Figure 1. The temperature dependence of the line shape of ESR spectra is due to the change in the motional correlation time, τ_c, of the nitroxides. The outermost splitting width between arrows in Figure 1 of the main triplet spectrum due to hyperfine coupling caused by the nitrogen nucleus narrows with an increase in mobility of the radicals because of motional averaging of the anisotropic interaction between an electron and a nucleus. The complete averaging gives rise to the isotropic narrowed spectrum. Two spectral components, a "fast" and a "slow" component, are observed in the temperature-dependent ESR spectra of the labeled HDPE or LDPE. In general, the two spectral components are observed in a certain temperature range for crystalline polymers, polymer blends, block and graft copolymers, etc.[24−32] The slow component with the large

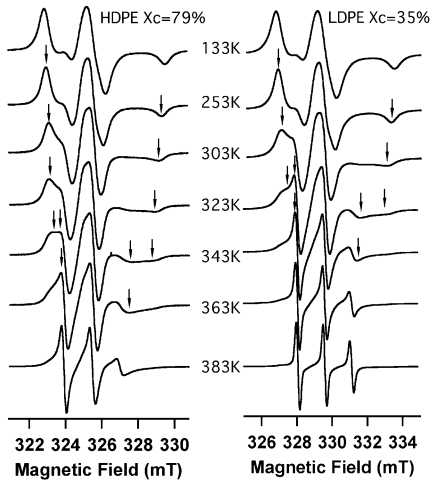

Figure 1. Temperature-dependent ESR spectra of the HDPF with X_c of 79% and LDPE with X_c of 35%. The width between arrows indicates the outermost splitting.

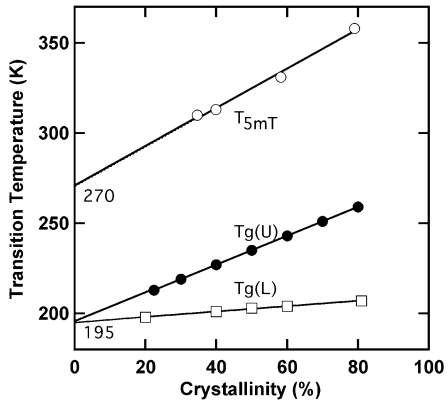

Figure 2. Crystallinity dependence of transition temperature. Open circles indicated T_{5mT} observed from ESR. Solid circles and squares measured by a thermal expansion were referred from the literature.

outermost splitting width and the fast component with small outermost splitting width and narrow line width can be attributed to radicals in less mobile and mobile regions, respectively. This is a reflection of a broad distribution of the τ_c arising from a heterogeneous structure in the polyethylene. It is indeterminable whether the correlation time is bimodal or broad single distribution from only the ESR spectra. Both cases showed a bimodal behavior. Such ESR spectra indicate the system has inhomogeneous structure. It is, in addition, generally hard to extract two rotational correlation times from each spectrum without an appropriate spectral simulation. In this paper, the narrowing of the outermost splitting was used to analyze the transition temperature because the slow component is dominant in the ESR spectrum, at least below the transition temperature. The temperature where the outermost splitting of the spectrum is 5 mT is defined as a motional transition temperature T_{5mT}.

Figure 2 shows the X_c dependence of transition temperature T_{5mT} from the ESR method. The transition temperature clearly depended on X_c. Stehling and Manderkern measured a thermal expansion of linear polyethylene with different X_c.[4] Boyer replotted the amorphous relaxation (glass transition) data of Stehling and Manderkern as a function of X_c.[5] The temperatures estimated by Boyer are plotted in the figure to compare with our results. It was said that the T_g(U) and T_g(L) are arising from glass transition of the chain trapped in the different amorphous regions, meaning a heterogeneous structure of polyethylene. According to Boyer's papers, the upper transition temperature (labeled U) comes from the tie chain and lower (labeled L) transition comes from long loop chain and tail chain. In our study, two ESR spectral components (fast and slow components) may two phases in the amorphous region as Boyer mentioned. However, the detailed analysis of the mobile spectra below the transition temperature of the slow component was so difficult that the assignment of the fast component cannot be done here. Interestingly, the crystallinity dependence of T_{5mT} was very close to that of T_g(U), except for the transition temperature. The difference of these transitions is ascribed to a frequency difference between two observations. The extrapolated temperature to X_c of zero is implied as a transition temperature of "a perfect amorphous" polyethylene. The extrapolated temperatures estimated by us and Manderkern were 270 and 195 K, respectively. The τ_{ESR} at T_{5mT} is generally referred to 4.3×10^{-9} s.[33] The τ_g at the glass transition temperatures measured by a dilatometric method is 100 s.[34,35] The difference between transition temperatures, ΔT, can be estimated by WLF equation[36] for simplicity.

$$\log\left(\frac{\tau_{ESR}}{\tau_g}\right) = \frac{-17.44(T_{5mT} - T_g)}{51.6 + T_{5mT} - T_g}$$

One can obtain $\Delta T = T_{5mT} - T_g = 76$ K. From the WLF equation, the T_g from ESR is expected to be 194 K, which is close to the extrapolated T_g (195 K) to X_c of zero. Therefore, the molecular motion detected by the ESR spin-labeled method here is associated with the glass transition (β-relaxation, T_g(U)) proposed by Boyer et al.[5] The spin-labeled sites are likely located at the amorphous region because labeled segments are reasonable to be excluded from the crystalline region. Thus, it can be said that the labeled segments reflect the motion of amorphous segments. The crystallinity dependence of T_{5mT} is obtained as T_{5mT} (K) $= 1.1X_c + 270$. The effect of crystallinity on the mobility seems to be somewhat ambiguous. We considered, however, that the crystallinity effect on the mobility was "a mean effect" of various effects originated from various crystalline structures, such as a long period, crystalline size, and a fraction of tie molecules on the mobility, which might affect the mobility of the amorphous chains. A quantitative evaluation of the relation of the detailed crystalline structure with the mobility seems to be quite difficult. In this study, we treated the crystallinity as the mean effect.

Influence of Chain End on Molecular Motion of PE. Figure 3 shows temperature-dependent ESR spectra of inner-labeled HPB (left) with the M_n of 30 000 and the X_c of 40.3% and end-labeled E-HPB (right) with the M_n of 29 300 and the X_c of 39.7%. They clearly indicate different temperature dependence. As compared with the spectra observed at 333 K, for example, the mobile fraction in the spectrum for E-HPB was larger than that for inner-labeled HPB, meaning the end-labeled E-HPB has higher mobility. As reported in amorphous polymers,[22,23] this is because that the segment around the chain end includes a large free volume relative to the segment around inside segments. Figure 4 shows the transition temperatures detected by ESR and by MDSC of spin-labeled HPB, E-HPB, and PE with

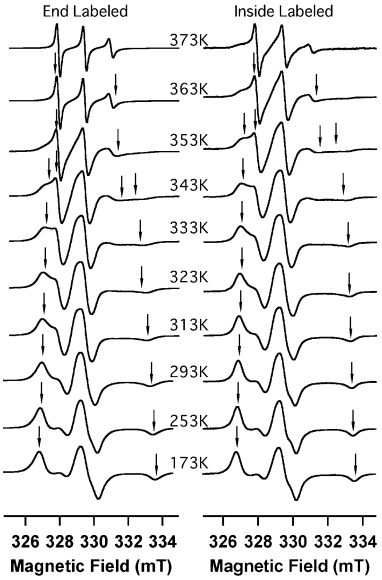

Figure 3. Temperature-dependent ESR spectra of inner-labeled HPB (left) with the M_n of 30 000 and the X_c of 40.3% and end-labeled E-HPB (right) with the M_n of 29 300 and the X_c of 39.7%.

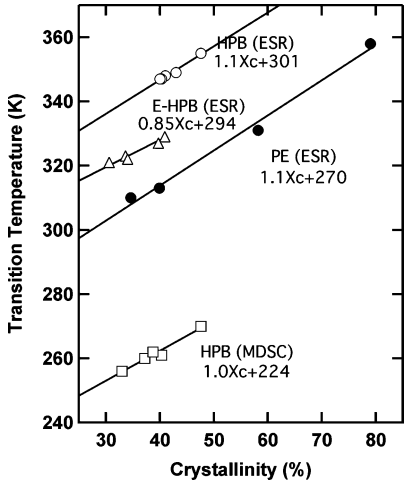

Figure 4. Transition temperatures detected by ESR and MDSC of spin-labeled HPB (open circles, T_{5mT}), E-HPB (triangles, T_{5mT}; squares, $T_{g,DSC}$), and PE (solid circles, T_{5mT}) with different X_c.

different X_c. The molecular weight of these polymers was over 20 000 where the M_n effect on T_g can be ignored. The slope of the lines fitted by a least-squares method means the X_c dependence of transition temperatures. The X_c dependence of T_{5mT} for HPB was about 1.1, which was almost equal to that of PE. The MDSC indicated almost the same dependence of T_g. On the other hand, the weaker X_c dependence for E-HPB was obtained to be 0.85. An inner chain segment in the amorphous region is generally connected to the crystalline to present as a loose long loop, short loop, and tie chains. However, a chain-end segment is preferentially tail state in the amorphous matrix. In other words, the inner segments are located necessarily near the crystalline in comparison with the end segments. The crystalline results in reducing the mobility of the inner segments and the X_c dependence of the labeled inner segments became strong.

As to inner-segment labeled PE and HPB, although the X_c dependence of the transition temperature was the same, the difference in extrapolated value to X_c of

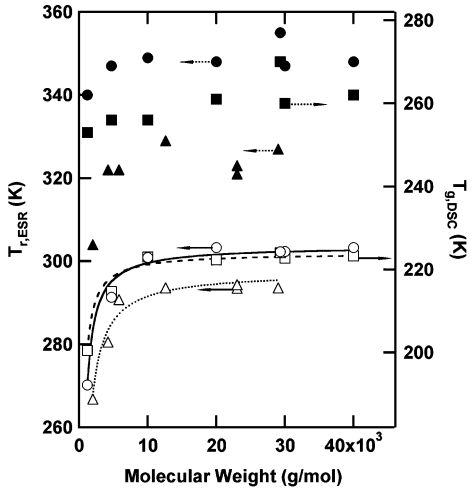

Figure 5. Plot of transition temperatures against the molecular weight, which were observed by ESR (circles for HPB and triangles for E-HPB) and DSC (squares). Solid and open symbols represent the raw and the reduce values, respectively. The lines represent $1/T_g = 1/T_{g\infty} + A/M_n$.

zero between HPB and PE (HDPE and LDPE) were found. The transition temperature of HPB at fully amorphous state (when $X_c = 0$) was higher than PE (LDPE and HDPE). This discrepancy can be explained as follows. It is caused by effect of relatively high fraction of the ethyl branch in HPB. The short branch such as ethyl branch is excluded from the crystalline, which was revealed by solid-state NMR.[37] Therefore, ethyl branches are enriched in the amorphous region by the crystallization. The glass transition temperature of amorphous poly(ethylethylene) was reported to be 240 K,[38] which is higher than the β-transition (195 K) of a linear polyethylene. The glass transition of HPB in the fully amorphous state, thus, can be expected to be in the range of 195−240 K. In fact, the extrapolated value to X_c of zero was estimated to be 224 K, which falls in within the expectable range and higher than the β-transition (195 K) of fully amorphous linear PE. On the other hand, the extrapolated value of HPB from ESR was 301 K. Taking into account the time scale, this value can be reduced to be 225 K at DSC time scale, which was identical with the extrapolated temperature from DSC measurement. The extrapolated T_{5mT} of E-HPB was estimated to be 294 K, which was lower than that of HPB (301 K), indicating that there are large free volume around the chain end segment which enhance the mobility. A larger specific free volume around chain ends and higher mobility around end segments than that around inside segments has been reported by other researcher's works using other techniques such as a photolabel method[39] and a positron annihilation lifetime technique,[40] which is consistent with our results.

Molecular Weight Dependence of Transition Temperature. To investigate the molecular weight dependence of molecular mobility, a series of HPB with different M_n were prepared. In Figure 5, the transition temperatures are plotted against the molecular weight, which were observed by ESR and MDSC. Filled symbols mean raw data (without reducing by crystallinity or observation frequency). Raw data show the slight molecular weight dependence, but it is obscured by the crystallinity dependence. First, the influence from crystallinity was eliminated using the relation between X_c and transition temperature obtained from Figure 4. To compare the data from ESR and DSC, ESR transition

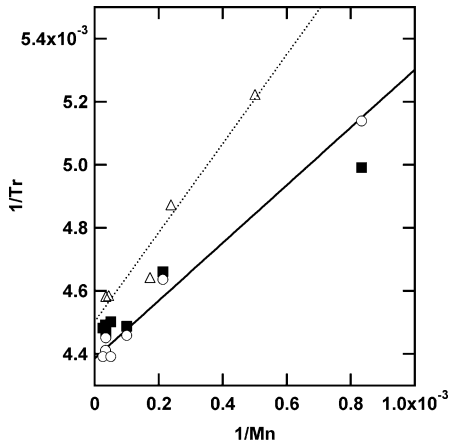

Figure 6. Molecular weight dependence of $T_{r,i}$ (circles), $T_{r,e}$ (triangles), and $T_{g,DSC}$ (squares) of hydrogenated PB. The lines represent $1/T_g = 1/T_{g\infty} + A/M_n$.

temperatures were reduced to the temperatures at time scale of 100 s (DSC)[34,35] using the WLF equation. Open symbols indicate the reduced values according to both the X_c dependence of transition temperature and WLF equation. Transition temperatures of inner (open circles, denoted as $T_{g,i}$) and end segments (open triangles, denoted as $T_{g,e}$) from ESR and DSC (open squares, denoted as $T_{g,DSC}$) clearly show a molecular weight dependence. The drawn lines obey the Ueberreiter−Kanig relation ($1/T_g = 1/T_{g\infty} + A/M_n$).[41,42] The M_n dependence of transition temperature from ESR and DSC was almost identical with each other, meaning also that ESR measurement studied here represented glass transition phenomenon. The inverse of the $T_{g,i}$, $T_{g,e}$, and the $T_{g,DSC}$ are plotted against the reciprocal of the M_n (Figure 6). The linear relationship of eq 1 gives $T_{g\infty,i}$ and A_i to be 228 K and 0.91, respectively. $T_{g\infty,e}$ and A_e were determined to be 222 K and 1.4, respectively. The M_n dependence of the $T_{g,e}$ suggests that the $T_{g,e}$ reflected the β relaxation of the PE, not the other local motions which occur at lower temperature than β relaxation because the local motions might have no molecular weight dependence. In addition, the M_n dependence of the $T_{g,e}$ indicates the cooperative motion[43] of chain end segments with neighboring inside segments. In other words, the cooperative motion with neighboring segments is considered to be necessary for not only inside segments but also chain end segments to undergo a rotational relaxation. Therefore, the molecular weight dependence of the $T_{g,e}$ can be interpreted in terms of the influence of the neighboring inside segments.

The A_e was roughly 1.5 times larger than the A_i. The larger A_e than the A_i indicates the strong molecular weight dependence on the mobility around chain ends, namely, the mobility around chain ends is more enhanced than that of inside segments with a decrease in the molecular weight. This behavior was previously observed for PS[22] and PMMA.[23] These results are interesting to understand dynamic features of chain ends. In the previous paper, a simple model on the basis of the probability of an encounter of chain ends was suggested to interpret the strong molecular weight dependence of the $T_{g,e}$.[22] As described above, the cooperative motion with neighboring segments is necessary in the bulk when a segment undergoes β-relaxation. This model bases on an idea that the encounter of chain ends locally increases mobility around them. In this model, it is assumed that one noticed segment is surrounded with four other segments. The combination of an arrangement of each segment in this situation is considered. Four surrounding segments consist of four polymeric chains including eight end segments. When the number of the segments in one polymeric chain, n, is large, the probability (concentration) that the noticed segment is surrounded with four inside segments is calculated to be approximately $1 - 8/n$, as mentioned in detail in our previous paper.[22,23] Similarly, $8/n$ is obtained approximately for the probability that the noticed segment is surrounded with three inside and one end segments. The other probabilities can be ignored because they are relatively too small. The Doolittle equation is the most relevant to relate a relaxation rate to a free volume fraction, f

$$1/\tau_c = A_d \exp(-B/f) \tag{1}$$

Here, A_d and B are constants. In the concept of iso-free volume, the free volume fraction f is almost 0.025 at T_g. At each arrangement, a local free volume fraction $f_k = f + \Delta f_k$, where Δf_k is the deviation from the average f. It can be expected commonly that each local free volume fraction of each arrangement is not so different, i.e., $\Delta f_k/f \ll 1$. In this condition, the following relation can be formed approximately.

$$1/f \sim \sum_k (P_k/f_k), \quad \sum_k P_k = 1 \tag{2}$$

P_k and f_k are the probability (concentration) and the local free volume fraction of each arrangement (site k), respectively. Substituting eq 2 into eq 1, one obtains

$$\ln(1/\tau_c) = \ln A_d - B\sum_k (P_k/f_k) \tag{3}$$

According to eq 1

$$1/\tau_{c,k} = A_d \exp(-B/f_k) \tag{4}$$

Combining eqs 3 and 4, one can obtain

$$\ln(1/\tau_c) = \sum_k P_k \ln(1/\tau_k) \tag{5}$$

Therefore, the average relaxation rate can be expressed by eq 5. In the assumption that each local free volume is not so different, the above relation can be held. When a chain end segment is surrounded with four segments, the average relaxation rate ($1/\tau_e$) of the spin-labels at the chain end could be given as[22,23]

$$\ln(1/\tau_e) = (1 - 8/n)\ln(1/\tau_{e-i_4}) + (8/n)\ln(1/\tau_{e-i_3e_1}) = 8[\ln(1/\tau_{e-i_3e_1}) - \ln(1/\tau_{e-i_4})]/n + \ln(1/\tau_{e-i_4}) \tag{6}$$

Here, τ_{e-i_4} is the relaxation time in the case that the end segment is surrounded with four inside segments. $\tau_{e-i_3e_1}$ expresses the relaxation time that the end segment is surrounded with one end and three inside segments. Similarly, the average relaxation rate of the spin-labels at the inside of the chain ($1/\tau_i$) is expressed by

$$\ln(1/\tau_i) = (1 - 8/n)\ln(1/\tau_{i-i_4}) + (8/n)\ln(1/\tau_{i-i_3e_1}) = 8[\ln(1/\tau_{i-i_3e_1}) - \ln(1/\tau_{i-i_4})]/n + \ln(1/\tau_{i-i_4}) \tag{7}$$

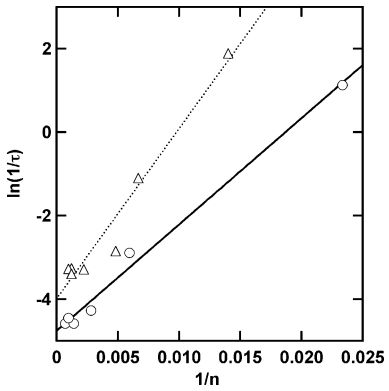

Figure 7. Plot of $\ln(1/\tau_i)$ (circles) and $\ln(1/\tau_e)$ (triangles) against the reciprocal of degree of polymerization n. The data were fitted with $\ln(1/\tau_i) = 255/n - 4.76$ and $\ln(1/\tau_e) = 408/n - 3.99$ obtained by the least-squares method.

The n was first defined as a degree of polymerization to compare the eqs 3 and 4 with experimental results for simplicity. The $\ln(1/\tau_i)$ and $\ln(1/\tau_e)$ determined from the experiment were plotted against the inverse of the n, and the data were fitted with linear relation according to eqs 3 and 4 in Figure 7. Here, the τ_i and τ_e were calculated using WLF equation with the reference temperature 228 K with $\tau_c = 100$ s and the ESR transition temperatures at X_c of zero (reduced ones), i.e., the calculated τ is regarded as the correlation time at X_c of zero. The intercept terms of the fitted lines give the τ_{i-i_4} and τ_{e-i_4} to be ca. 100 and 53 s, respectively. When the segment size related to the cooperative motion is taken into account, it is actually inappropriate to refer the degree of polymerization as the segmental unit. The actual number of motional segment per chain, a, can be expressed by $a = n/x$, where x is the number of monomer unit involved in the segmental motion at T_g. The n should be substituted with a in eqs 6 and 7. Therefore, eqs 6 and 7 should be represented again by

$$\ln(1/\tau_e) = 8x[\ln(1/\tau_{e-i_3e_1}) - \ln(1/\tau_{e-i_4})]/n + \ln(1/\tau_{e-i_4}) \quad (8)$$

$$\ln(1/\tau_i) = 8x[\ln(1/\tau_{i-i_3e_1}) - \ln(1/\tau_{i-i_4})]/n + \ln(1/\tau_{i-i_4}) \quad (9)$$

When it is assumed that the τ_{e-i_4} can be approximately equal to the $\tau_{i-i_3e_1}$, the x is estimated 42 from the slope of the fitted line and eq 9. The motional volume v_{seg} (segment volume) of PE can be calculated roughly using the x, the mass m_r of PE repeat unit, and the density ($d = 0.855$ g/cm^3) of amorphous PE.[38] The volume v_s ($= xm_r/d$) of one segment was estimated to be 2.3 nm^3 at glass transition. According to Lodge et al.,[44] the cooperative volume above the glass transition is comparable to the cube of the Kuhn length, l_k, which is defined as $C_\infty l$. C_∞ is the characteristic ratio, and l is the length of the average backbone bond. As the C_∞ of PE is 6.7,[45] the l_k is 1.02 nm. Thus, the l_k^3 is obtained to be ca. 1.1 nm^3, which is the same order with the estimated v_s. We obtained previously that the v_s of PS,[22] poly(cyclohexyl methacrylate),[46] and PMMA[23] determined by the same procedure were in good agreement with the respective l_k^3. Even in the case of PE, the result is consistent with previous works. But the l_k^3 is presumably independent of temperature.[47] In contrast, the cooperative rearrangement regions $v_{CRR} = \xi^3$ is assumed to diverge at the Vogel temperature, i.e., temperature dependent. The

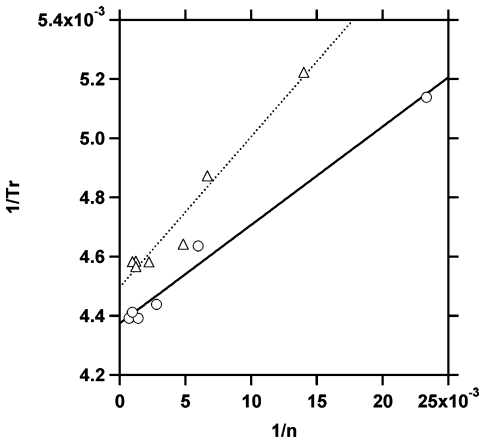

Figure 8. Plot of $1/T_{gi}$ (circles) and $1/T_{ge}$ (triangles) against the reciprocal of degree of polymerization n. The data were fitted with $1/T_{gi} = 0.0323/n + 0.00437$ and $1/T_{ge} = 0.0509/n + 0.0450$ obtained by the least-squares method.

volume estimated in this study is essentially related to the glass transition. The characteristic length ξ of glass transition corresponds to the size of cooperative rearranging regions of Adam and Gibbs ξ.[3,48] The length ξ was reported to be a few nanometers by Donth et al.[49] In this study, the monomer volume v_m of PE was assumed to be m_r/d. The monomer size (length) l_m can be defined as $v_m = (4/3)\pi(l_m/2)^3$. Assuming that the characteristic length ξ is the average end-to-end distance of the PE chain with $x = 42$, the ξ was calculated to be 1.9 nm with $\xi = l_m x^{1/2}$, which was within the reported ξ for various polymers.

The finding of x gives the $\tau_{e-i_3e_1}$. It was calculated to be 16 s. This is induced by the much larger free volume generated by two chain ends. A decrease in the molecular weight leads to an increase in the number of chain ends. As a result, the probability of the encounter of two chain ends increases. The encounter of the end segment shortened the relaxation time. As the molecular weight decreases, the T_g in the region near the chain end is steeply depressed.

Another way to interpret this molecular weight dependence of inner and end segments is considered. One can treat the average transition temperature of a miscible polymer blend using the Fox-type equation as a first approximation

$$1/T_r = \sum_k (P_k/T_k)$$

Similarly, the inversion of the average transition for inner and end segments can be given by

$$1/T_i = 8x[1/T_{i-i_3e_1} - 1/T_{i-i_4}]/n + 1/T_{i-i_4} \quad (10)$$

$$1/T_e = 8x[1/T_{e-i_3e_1} - 1/T_{e-i_4}]/n + 1/T_{e-i_4} \quad (11)$$

respectively. Here, T_{i-i_4} and T_{e-i_4} are the transition temperatures in the case that the noticed segment is surrounded with four inside segments. $T_{i-i_3e_1}$ and $T_{e-i_3e_1}$ express the relaxation time that the noticed segment is surrounded with one end and three inside segments. Equations 10 and 11 represent the same form as the Ueberreiter−Kanig equation. In Figure 8, the inverse of the transition temperatures are repotted as a function of $1/n$. Similar analysis gives the $T_{e-i_3e_1}$ and the number of the segments moved cooperatively at T_g to be 214 K

and 35, respectively. According to the time−temperature superposition, the transition temperature of 214 K corresponds the correlation time of about 13 s, which is close to the $\tau_{e-i_3e_1}$. The v_s and ξ can be calculated to be 1.9 nm^3 and 1.8 nm, respectively, which also coincide with the previous one. Note that if the average of the transitions using simple Gordon−Taylor equation is considered, the M_n dependence of the transition temperature results in the same form as the case of the Fox equation. In that case the $T_{e-i_3e_1}$, $\tau_{e-i_3e_1}$, n, v_s, and ξ are obtained to be 212 K, 10 s, 29, 1.6 nm^3, and 1.6 nm, respectively. We think that these values are almost identical within the error to interpret the phenomena in this kind of study. Here, we make no mention which equations are proper and appropriate.

Conclusion

We evaluated the transition temperature detected by the spin-labeled ESR method. The transition measured by ESR corresponded to the β transition which can be treated as a glass transition phenomenon. The transition temperature of semicrystalline polymer, PE, was found to depend on the crystallinity, the molecular weight of the sample, and the labeled site such as inner or end segments. The β relaxation around chain-end segments was observed by the selective spin-labeling method, and it was revealed to depend on the molecular weight of the sample as well as the inner segments. In addition, the size of cooperative length, which related to cooperative segment motion, of PE at T_g was estimated to be around 2 nm, which is the same order as the ξ for various polymers and the Kuhn length of PE.

Acknowledgment. Thanks are due to the Research Center for Molecular-Scale Nanoscience, the Institute for Molecular Science, for assistance in obtaining the MDSC data. The SAXS and WAXD measurements were performed under approval of the Photon Factory Program Advisory Committee (Proposal 2001G275). This research was partially supported by the Ministry of Education, Science, Sports and Culture, Grant-in-Aid for Young Scientists (B), 16750185, 2004.

References and Notes

(1) Boyer, R. F. *Rubber Chem. Technol.* **1963**, *36*, 1303.
(2) McCrum, N. G.; Read, B. E.; Williams, G. *Anelestic and Dielectric Effects in Polymer Solids*; John Wiley & Sons: New York, 1965.
(3) McKenna, L. W.; Kajiyama, T.; MacKnight, W. J. *Macromolecules* **1969**, *2*, 58.
(4) Stehling, F. C.; Manderkern, L. *Macromolecules* **1970**, *3*, 242.
(5) Boyer, R. F. *Macromolecules* **1973**, *6*, 288.
(6) Ohlberg, S. M.; Fenstermaker, S. S. *J. Polym. Sci.* **1958**, *32*, 514.
(7) Culter, D. J.; Glotin, M.; Hendra, P. J.; Jobic, H. *J. Polym. Sci., Polym. Phys. Ed.* **1979**, *17*, 907.
(8) Rabold, G. P. *J. Polym. Sci., Part A-1* **1969**, *7*, 1203.
(9) Lin, D.; Wang, S. J. *J. Phys.: Condens. Matter* **1992**, *4*, 3331.
(10) Schurr, O.; Yamaki, B. S.; Wang, C.; Atvars, T. D. Z.; Weiss, R. G. *Macromolecules* **2003**, *36*, 3485.
(11) van der Berg, O.; Sengers, W. G. F.; Jager, W. F.; Picken, S. J.; Wübbenhorst, M. *Macromolecules* **2004**, *37*, 2460.
(12) Boyer, R. F. *J. Macromol. Sci., Phys.* **1973**, *B8*, 503.
(13) Kanaya, T.; Buchenau, U.; Koizumi, S.; Tsukushi, I.; Kaji, K. *Phys. Rev. B* **2000**, *61*, R6451.
(14) de Langen, M.; Luigjes, H.; Prins, K. O. *Polymer* **2000**, *41*, 1183.
(15) Yamamoto, S.; Tsujii, Y.; Fukuda, T. *Macromolecules* **2002**, *35*, 6077.
(16) Blum, F. B.; Liang, M.; Wade, C. G. *Macromolecules* **1996**, *29*, 8740.
(17) (a) Yamamoto, K.; Maruta, A.; Shimada, S. *Polym. J.* **2001**, *33*, 584. (b) Shimada, S.; Maruta, A.; Yamamoto, K. *Polym. J.* **2000**, *32*, 1038.
(18) Miwa, M.; Tanida, K.; Yamamoto, K.; Okamoto, S.; Sakaguchi, M.; Sakai, M.; Makita, S.; Sakurai, S.; Shimada, S. *Macromolecules* **2004**, *37*, 3707.
(19) Morèse-Séguéla, B.; St-Jacques, M.; Renaud, J. M.; Prud'homme, J. *Macromolecules* **1980**, *13*, 100.
(20) Dollase, T.; Graf, R.; Heuer, A.; Spiess. H. W. *Macromolecules* **2001**, *34*, 298.
(21) Kitamaru, R.; Horii, F.; Maruyama, K. *Macromolecules* **1986**, *19*, 636.
(22) Miwa, Y.; Tanase, T.; Yamamoto, K.; Sakaguchi, M.; Sakai, M.; Shimada, S. *Macromolecules* **2003**, *36*, 3235. In the previous paper,[22,23] the approximation of the probability (concentration) that the noticed segment surrounded with four inside segments was miscalculated. It was calculated to be approximately $1 - 9.5/n$, which was wrong. The corrected probability is $1 - 8/n$ as described in this article.
(23) Miwa, Y.; Yamamoto, K.; Sakaguchi, M.; Sakai, M.; Makita, S.; Shimada, S. *Macromolecules* **2005**, *3*. 832.
(24) Schlick, S.; Harvey, R. D.; Alonso-Amigo, M. G.; Klempner, D. *Macromolecules* **1989**, *22*, 822.
(25) Miwa, Y.; Yamamoto, K.; Sakaguchi, M.; Sakai, M.; Tanida, K.; Hara, S.; Okamoto, S.; Shimada, S. *Macromolecules* **2004**, *37*, 831.
(26) Aras, L.; Richardson, M. J. *Polymer* **1989**, *30*, 2246.
(27) Cameron, G. G.; Qureshi, M. Y.; Tavern, S. C. *Eur. Polym. J.* **1996**, *32*, 587.
(28) Brown, I. M. *Macromolecules* **1981**, *14*, 801.
(29) Shimada, S.; Kozakai, M.; Yamamoto, K. *Polymer* **1998**, *32*, 6013.
(30) Varghese, B.; Schlick, S. *J. Polym. Sci., Part B: Polym. Phys.* **2002**, *40*, 415.
(31) Cameron, G. G.; Qureshi, M. Y.; Stewart, D.; Buscall, R.; Nemcek, J. *Polymer* **1995**, *36*, 3071.
(32) Cameron, G. G.; Stewart, D. *Polymer* **1996**, *37*, 5329.
(33) Goldman, S. A.; Bruno, G. V.; Freed, J. H. *J. Phys. Chem.* **1972**, *76*, 1858.
(34) Angell, C. A. *J. Non-Cryst. Solids* **1991**, *131−133*, 13.
(35) Ngai, K. L.; Plazek, D. J. *Rubber Chem. Technol.* **1995**, *68*, 376.
(36) Williams, M. L.; Landel, R. F.; Ferry, J. D. *J. Am. Chem. Soc.* **1995**, *77*, 3701.
(37) Kuwabara, K.; Kaji, H.; Horii, F.; Bassett, D. C.; Olley, R. H. *Macromolecules* **1997**, *30*, 7516.
(38) *38.Polymer Handbook*, 4th ed.; Wiley-Interscience: New York, 1999.
(39) (a) Yu, W.; Sung, C. S. P.; Robertson, R. E. *Macromolecules* **1988**, *21*, 355. (b) Yu, W.; Sung, C. S. P. *Macromolecules* **1988**, *21*, 365.
(40) Li, H.; Ujihira, Y.; Nanasawa, A. *Kobunshi Ronbunshu* **1996**, *53*, 358.
(41) Ueberreiter, K.; Kanig, G. *J. Colloid Sci.* **1952**, *7*, 569.
(42) Fox, T. G.; Loshaek, S. *J. Polym. Sci.* **1955**, *15*, 371.
(43) Matsuoka, S.; Quan, X. *Macromolecules* **1991**, *24*, 2770.
(44) Lodge, T. P.; McLeish, T. C. B. *Macromolecules* **2000**, *33*, 5278.
(45) Strobl, G. *The Physics of Polymers*, 2nd ed.; Springer: Berlin, 1997.
(46) Miwa, Y.; Sugino, Y.; Yamamoto, K.; Tanabe, T.; Sakaguchi, M.; Sakai, M.; Shimada, S. *Macromolecules* **2004**, *37*, 6061.
(47) Kant, R.; Kumar, S. K.; Colby, R. H. *Macromolecules* **2003**, *36*, 10087.
(48) Adam, G.; Gibbs, J. H. *J. Chem. Phys.* **1965**, *43*, 139.
(49) Hempel, E.; Hempel, G.; Hensel, A.; Schick, C.; Donth, E. *J. Phys. Chem. B* **2000**, *104*, 2460.

MA050062F